Plant compartments and developmental stages modulate the balance between niche-based and neutral processes in soybean microbiome

Moroenyane, I[a]., Mendes, L[b]., Tremblay J[c]., Tripathi, B[d], and Yergeau, É[a]*

a) Institut National de la Recherche Scientifique, Centre Armand-Frappier Santé Biotechnologie, 531 Boulevard des Prairies, Laval, Québec, H7V1B7, Canada
b) Center for Nuclear Energy in Agriculture, University of São Paulo, Piracicaba, SP 13400-970, Brazil
c) Energy, Mining, and Environment, National Research Council Canada, 6100 Avenue Royalmount, Montreal, Quebec, H4P 2R2, Canada
d) Korea Polar Research Institute, Incheon, 21990, Korea

Keywords: Soybean Microbiome, Niche-based assembly, Community Assembly, Phylogenetic community structure

Running title: Assembly processes in soybean microbiome

***Corresponding authors:** É.Yergeau
Tel: 450-687-5010; Email: etienne.yergeau@ inrs.ca

Abstract

Understanding the dynamics of plant-associated microbial communities within agriculture is well documented. However, the ecological processes that assemble the plant microbiome are not well understood. This study elucidates the relative dominance of assembly processes across plant compartments (root, stem, and leaves) and developmental stages (emergence, growth, flowering, and maturation). Bacterial community composition and assembly processes were assessed using 16S rRNA gene amplicon sequencing. Null models that couple phylogenetic community composition and species distribution models were used to evaluate ecological assembly processes of bacterial communities. All models highlighted that the balance between the assembly process was modulated by compartments and developmental stages. Dispersal limitation dominated amongst the epiphytic communities and at the maturation stage. Homogeneous selection dominated assembly across plant compartments and developments stages. Overall, both sets of models were mostly in agreement in predicting the prevailing assembly processes. Our results show, for the first time, that even though niche-based processes dominate in the plant environment, the relative influence of dispersal limitation in community assembly is important.

Introduction

Microbial communities that colonise plant surface from the roots to the leaves and the inside of plant organs help overcome abiotic stress [1]. The colonisation, diversity, and succession patterns of these microbial communities have become a research focus of interest for ecologists, including efforts to identify and include microbial communities in sustainable agricultural practices [2, 3]. One of the prerequisites to such efforts is to understand the ecological processes that delimit microbiomes across plant compartments and growth stages, not only at the root-soil interface [3, 4]. Ecological communities are assembled simultaneously by both niche-based (environmental filtering) and neutral processes (dispersal limitations, ecological drift, and speciation events)[5, 6]. However, the dominance of these processes across developmental stages and plant compartments within a single genotype remains unknown.

Fundamentally, plant microbial communities are defined by 1) their taxonomic compositions, 2) functional capacity, and 3) dominance of assembly processes. These inherent community characteristics are influenced by plant genotype[7] , plant species [8] , and plant nutrient status[9]. These studies have highlighted that there is an interaction between the different components of the microbiomes. For instance, microbial taxa in the rhizosphere tend to influence community assembly processes by modulating the expression of crucial plant functional genes [10, 11], and assembly processes within rhizosphere microbiome vary across crops [12].

Essentially, there are two classes of models from which community assembly can be inferred. Firstly, phylogenetic null models (PNM), where the integration of phylogenetic and species pool data has led to a framework from which mechanisms of community assembly can be

inferred [13, 14]. At their core, these approaches combine a phylogenetic community structure index such as beta mean nearest taxon distance (βMNTD) which estimates phylogenetic turnover between assemblages[15, 16] and null models to quantify deviation from null expectations[15, 17, 18]. The null model randomly shuffles the taxa across tips of the phylogenetic tree and βMNTD is recalculated, and this provides one null value for βMNTD[15, 19]. After several rounds of iterations, the model provides a distribution of βMNTD values and deviations between the observed βMNTD value and null βMNTD distributions are quantified as ß-nearest taxon index (βNTI)[15, 20]. Niche-based selection imposed by the environment are then quantified as 1) homogenous selection (βNTI less than 2) implies that selective pressure exerted by the environment is spatially homogenous and does not significantly change between periods, 2) heterogeneous selection (βNTI greater than 2) implies that the selective pressure changes between periods [20]. Under homogenous selection, taxa that are selected at a specific period will be continuously selected; whereas, under heterogeneous selection, different taxa will be selected across different periods. These models have been used to quantify the relative influence of different assembly processes [4] to predict niche constraints of soil microbes [21] and to elucidate microbial biogeographical patterns[22, 23]. Secondly, species distribution models (SDM) use taxonomic composition and niche-based or neutral assembly models to predict the prevailing assembly processes. Typically, niche-based SDM models predict that changes in species abundance and distribution are interconnected to changes in environmental conditions (environmental filtering) [24, 25]. These models aim to describe the abundance distribution of taxa given the occupied niche space. Broadly, these models predict how taxa that occupy similar niche spaces can coexist by niche partitioning [26-28]. Under niche-based assembly, niche partitioning within communities can be modelled with several models: 1) broken stick, pre-emption, log-normal, and Zipf-

Mandlebrot [25, 29]. Species distribution models use abundance and distribution of taxa to quantify niche partitioning. Conversely, neutral SDM models predict that the abundance and distribution of taxa is a direct consequence of dispersal limitation and species abundance [30, 31]. The zero-sum model (ZSM) predicts that the abundance and distribution of taxa into niche spaces will be dominated by neutral processes [30, 32]. Similar to PNM models, SDM models have been useful in predicting soil microbial biogeographical patterns [33], soybean rhizosphere taxonomic and functional patterns [34, 35], and predict the composition of fungal leaf communities [36].

To date, studies that have elucidated community assembly processes within plant microbiomes have used either of these approaches and have focused mainly on a single plant compartment or developmental stage. Here, we were interested in using both PNMs and SDMs to quantify assembly processes of soybean microbiomes across spatial (plant compartments) and temporal (developmental stages) scales. We focused on elucidating assembly processes in soybean plants growing in pots under controlled growth chamber experimental conditions. Using the phylogenetically conserved regions of the 16S rRNA marker gene, we aimed at 1) elucidating the relative dominance of neutral and niche-based processes in assembling the plant bacterial community along spatial and temporal axes, and 2) comparing different complementary approaches to model assembly processes.

Methods

Plant growth conditions and microbiome sampling

Plants were grown in a Conviron growth chamber (Winnipeg, Canada), and were destructively sampled at the following developmental stages: V1 (emergence), V3 (growth), R1 (flowering), and R3 (maturation). The soil was collected in autumn of 2017 from an experimental field that had no history of agricultural practice, passed through a 40 mm sieve, and homogenised prior to potting. Soil analyses were performed in October 2017 by AgroEnviro Lab (La Pocatiere, QC) and revealed an average pH of 7.2, P concentration of 193 (kg/ha), total N 0.15%, C/N of 13.1 and other soil properties reported in Table S1. Plants were supplemented with a modified Hoagland's plant nutrient solution weekly [37]. A total of five plants were destructively sampled at each developmental stage, and DNA extraction was performed right after sampling. Samples were collected from rhizosphere, root, stem, and leaves. At each sampling period, the rhizosphere samples were considered as all the soil that was directly attached to the root surface. The entire epiphytic community (leaves, stem, and roots) was extracted using a modified protocol from Qvit-Raz, Jurkevitch and Belkin [38]. Briefly, the samples were placed in sterile 50 ml plastic Falcon test tubes (Corning, Tewksbury, MA, USA) and filled with sterile phosphate-buffered saline (PBS 0.1M, pH 7.4). The samples were then placed in a sonication tub (Fisher FS20, Fisher Scientific, Waltham, USA) for 15 min and vortexed for 10 s. The samples were then transferred into a new tube containing PBS and rinsed twice. The wash was pooled and spun down in a centrifuge at 2,000 g for 20 min, and the resulting pellet was considered to be the epiphytic community. The endophyte community was considered to be all the remaining microbes after the sonication and rinse treatment. Plant tissue was then pulverised in liquid nitrogen using a sterile pestle and mortar.

For each sample, 0.25 g was added to the bead tubes from the Qiagen Power Soil DNA kit (Hilden, Germany) and DNA was extracted following the manufacturer's instructions.

16S rRNA gene amplification and sequencing

The bacterial/archaeal V2-V3 hypervariable regions of the 16S rRNA gene were amplified using 520F and 799R primer pairs, which were shown to exclude chloroplast sequences [39]. The average lengths of 16S amplicon sequences were of approximately 280 bp. Briefly, extracted DNA was used to construct sequencing libraries according to Illumina's "16S Metagenomic Sequencing Library Preparation" guide (Part # 15044223 Rev. B), with the exception of using Qiagen HotStar MasterMix for the first PCR ("amplicon PCR") and halving reagent volumes for the second PCR ("index PCR"). The first PCR ("amplicon PCR") was carried out for 25 cycles with annealing temperatures of 55 °C. The resulting amplicons were pooled together and sequenced at the McGill University and Genome Québec Innovation Center (MUGQIC). Diluted pooled samples were loaded on an Illumina MiSeq and sequenced using a 500-cycle (paired-end sequencing configuration of 2x250 bp) MiSeq Reagent Kit v3. In total, 4,851,927 16S rRNA gene reads were received. Reads were processed using the AmpliconTagger pipeline [40, 41]. Briefly, raw reads were scanned for sequencing adapters, and PhiX spike-in sequences and remaining reads were merged using their common overlapping part with FLASH [42]. Primer sequences were removed from merged sequences, and remaining sequences were filtered for quality such that sequences having an average quality (Phred) score lower than 27 or one or more undefined base (N) or more than 10 bases lower than quality score 15 were discarded. Remaining sequences were clustered at 100% identity and then clustered/denoised at 99% identity (DNACLUST v3) [43]. Clusters having abundances lower than 3 were discarded. Remaining clusters were scanned for chimeras with

VSEARCH's version of UCHIME denovo [44], UCHIME reference [45], and clustered at 97% (DNACLUST) to form the final clusters/OTUs. OTUs were then assigned a taxonomic lineage with the RDP classifier [46], using the AmpliconTagger 16S training sets [47], respectively. The RDP classifier gives a score (0 to 1) to each taxonomic depth of each OTU. Each taxonomic depth having a score >= 0.5 was kept to reconstruct the final lineage. Multiple sequence alignment was then obtained by aligning the 16S rRNA gene OTU sequences on the SILVA R128 database [48] using the PyNAST v1.2.2 aligner [49]. Alignments were filtered to keep only the hypervariable region of the alignment. For cross-sample comparisons of alpha diversity, ten iterations were performed on a random subsample of 1,000 reads rarefactions, and the average number of reads of each OTU of each sample was then computed to obtain a consensus rarefied OTU table (Fig.S1). Samples represented by less than 1,000 reads were removed from the analyses (2 samples were removed). Alpha (observed species) and taxonomic summaries were then computed using the QIIME v1.9.1 software suite using the consensus rarefied OTU table[50, 51].

Statistical analyses

The OTU rank distribution for each sample was fit to niche-based models (null, pre-emption, log-normal, Zip f, and Mandelbrot) using the 'radfit' command in R [52], and neutral model (zero-sum model- ZSM) using TeTame v.2.1 [53] using the same OTU table used to construct the phylogenetic tree. The Akaike Information Criterion (AIC) was used to assess the relative quality of each model, and the model that had the lowest AIC value was considered the best fit model for the data [54, 55]. The AIC values for each model were calculated using the equation AIC= -2×log-likelihood+ 2×npar, where npar is the number of parameters used in the model[33, 36]. The statistical output is reported in Table 1. Dispersal rates were calculated by

Etienne's formula, using TeTame Software [53] (Table S3). Values of dispersal are between 0 and 1, where 0 means no tendency to migration and 1 means total tendency to migration in a specific community.

A maximum-likelihood tree was built from that all the aligned sequences of representative OTUs (a single representative sequence assigned to each OTU was used in subsequent analyses) with FastTree v2.1.10. using the GTR substitution model [56]. For cross-sample comparisons, the aligned fasta was subsampled to 1000 reads per samples, and samples with fewer than 1000s reads were discarded from all downstream phylogenetic analysis (Table S4; 26 samples were removed). Phylogenetic community turnover was evaluated using beta Nearest Taxon Index (βNTI) whose absolute magnitude reveals the relative influences of either niche-based or neutral processes. Briefly, using the mean nearest taxon index (MNTD), the standard effect size is calculated using the null mode 'taxa.labels' (999 randomisations in *Picante* [57]. The SES.MNTD index measures phylogenetic clustering in communities, with values >0 indicating phylogenetic overdispersion (distantly related taxa tend co-occur less than expected by chance) and values <0 indicating phylogenetic clustering (closely related taxa tend to co-occur more than expected by chance) [13]. The phylogenetic turnover across all communities was calculated as the beta MNTD (βMNTD). The βNTI index is calculated as the difference between the observed βMNTD and mean of the normalised (standard deviation) null distribution of βMNTD. βNTI values that are <-2 indicating significantly less than expected phylogenetic turnover whilst values >+2 indicating significantly more than expected phylogenetic turnover [16, 19, 20]. When βNTI values deviate from null expectation and value is between <-2 and >+2 it indicates the dominance of neutral processes [17], thus, observed differences in phylogenetic community compositions are the results of decreased dispersal rates (dispersal limitation), high dispersal rates (homogenising dispersal), or

undominated by a specific process. The Bray-Curtis based Raup-Crick (RC_{bray}) was used to determine the prevailing processes on pairwise comparison with βNTI values that lie between <-2 and >+2 [15, 20, 58]. Briefly, the contributions dispersal limitation was calculated as the percentage of pairwise comparisons with $|\beta NTI| < +2$ and $RC_{bray} > +0.95$, homogenising dispersal $|\beta NTI| < +2$ and $RC_{bray} < -0.95$, and those that did not fall into those categories indicated undominated selections. This randomisation holds constant the observed taxa richness, occupancy and, turnover. Thus, this technique provides the expected level of βNTI given observed richness, occupancy, and turnover [19]. A t-test was performed on the mean βNTI value to evaluate whether it significantly deviated from zero- which is expected under neutral assembly.

Sequence data deposition

The raw sequencing reads have been deposited in the NCBI SRA under Bioprect accession PRJNA601979: "Soybean microbiome - temporal and spatial development".

Results and discussion

To our knowledge, this is the first report that simultaneously provides evidence for the current assembly processes within bacterial niches across spatial and temporal axes in a controlled environment. Our aim to elucidate the overall processes within the plant microbiome highlighted that homogenous selection and dispersal limitations were the prevailing assembly processes across plant compartments and developmental stages. We were able to demonstrate that seemingly complementing approaches to quantifying assembly do reveal the dominance of similar processes across spatial and temporal axes, and these processes influence diversity patterns.

Overall, diversity patterns varied significantly across developmental stages and plant compartments. For instance, alpha diversity (OTU richness: developmental stage χ^2=12.37***; plant compartment χ^2=50.67***), beta diversity PERMANOVA (belowground: developmental stage R^2=0.21***, plant compartment R^2=0.25***; aboveground: developmental stage R^2=0.08***, plant compartment R^2=0.19***), and relative abundance of taxa at the phylum and order level varied significantly (Fig.S2). Recently, we demonstrated that these observed diversity patterns are modulated by interactions of spatial and temporal dynamics [59]. At a glance, the mean ßNTI value of the community significantly deviated from null expectations but was between <-2 and >+2 indicating the dominance of neutral processes (Fig.1 one sample t-test p<0.05). When disentangling the relative influence of different assembly processes, homogenous selection and dispersal limitation were the prevailing assembly processes across all plant compartments with heterogenous selection playing a minor role across all plant compartments : Leaf (endophyte μ = -0.52***; epiphyte μ = -0.21***), Stem (endophyte μ = -0.64***; epiphyte μ = -1.01***), Root (endophyte μ = -0.82***; epiphyte μ = -0.76***), and

Rhizosphere (μ = -0.14*) (Fig.1; Fig.S3). Phylogenetic beta diversity indices such as beta nearest taxon (ßNTI) show probabilistic (the likelihood of closely related taxa to co-occur less frequently than expected by chance) rather than absolute quantification of co-occurrences. This property of the models makes them ideal for detection of influences of environmental filtering rather than the nuanced ecological processes such as interspecific competition, for instance [60]. Equally, all species distribution models (SDMs) indicated that, for the abundance and distribution of communities, niche-based models were always the best model with the lowest Akaike Information Criterion (AIC) (Table 1; Fig. 2).

When nutrients are limiting, such as at the root-soil interface under certain conditions [61], there will be a more substantial influence of niche-based processes [62]. In soybean field trials, when micronutrients become limiting, there are increased dispersal rates across temporal axes [34]. Both PNMs and SDMs elucidated the dominance of niche-based selection (homogeneous) and increased dispersal at the root-soil interface (Fig.2; Fig.3; Fig.S3). This zone is a very selective environment [63], with rhizodeposition leading to the assembly of a microbial community in sharp contrast with bulk soil communities [10, 34, 35]. Also, it is possible that the reductionist experimental setup (i.e. closed chamber) significantly influenced the distribution and abundance of the bacterial community as detected by SDMs and increased dispersal rates within the epiphytic communities.

In contrast, SDM neutral assembly model had the best explanatory power for the assembly of the microbial communities of some leaf and root samples, suggesting that the plant selection stringency of these environments is relatively more relaxed. Successful colonisation of new bacterial niche spaces is predominantly dominated by species-sorting (niche-based) and dispersal limitation (neutral) [64]. The increased surface area of leaves and roots provides increases

dispersal opportunities for air-borne and free-living soil microbes to occupy these niche spaces, and dispersal limitation reinforces these current processes that occurred during initial colonisation [65]. The stem endosphere is a relatively nutrient-poor environment, or at least unbalanced, with a nitrogen content of sap directly affecting diversity and abundance of microbes [66, 67]. As such, homogenous selection dominated assembly at later developmental stages whilst heterogenous selection dominated at emergence (Fig.S3). We suggest that during the shorter developmental stages (emergence/flowering) the selective pressure asserted by the plant produces heterogeneous selection; whereas, at the longer reproductive stages (vegetative growth and maturation) homogeneous selection dominates.

For the growth stages, again, the mean ßNTI value of the epiphytic community significantly deviated from null expectations but was between <-2 and >+2 indicating the dominance of neutral processes: Emergence (μ = -0.21***), Growth (μ = -0.19***), Flowering (μ = -0.23***), Maturation (μ = -0.07***), and Overall (μ = -0.70) (Fig.4). On average, homogenising dispersal and selection (homogenous and heterogenous) processes accounted for majority assembly processes *ca.*60% at each developmental stage (Fig.5). Similarly, SDMs highlighted that neutral processes play a minor role in community assembly across other developmental stages (Fig.6). Generally, niche-based processes (homogenous and heterogenous) dominated at the growth and flowering stage, and dispersal dominated at the growth and maturation stages. It is proposed that as the plant's metabolic demand for nutrient and carbon increases at this stage, there will be a stringent selection for microbial taxa that can help in the provision of those nutrients [68, 69]. In the case of soybean, secondary metabolites (e.g. ethylamine and betaine) are produced during the flowering stage, and we suggest that the presence

295 of these molecules act as a robust environmental filter [68]. In fact, at the flowering stage, the
296 abundance and distribution were best predicted solely by the niche-based model despite increased
297 dispersal rates. It is then possible that within the communities, microbial taxa that were assembled
298 by neutral processes (speciation or drift) are competitively excluded due to their inability to
299 withstand strong environmental selection. These results presented here support observed
300 successional patterns of field- and laboratory-grown soybean plants, as we found the same
301 specialist taxa (Fig. S2) that characteristically dominate at different developmental stages in
302 soybean [69-71].
303 Dispersal rates varied across the plant compartment and developmental stages (Fig.3; Fig.5;
304 Fig.S3). The root and stem endophytic communities had a higher propensity for dispersal at the
305 flowering stage, whilst the leaf and stem epiphytic was during the growth stage. The leaf endophyte
306 and root epiphyte communities had increased dispersal rates at the maturation stage, whilst the
307 rhizosphere community has little to intermediate dispersal rates across all developmental stages.
308 For instance, SDMs neutral model had the best explanatory power for some communities at the
309 emergence, growth, and maturation stages, indicating that both neutral and niche-based processes
310 are essential in shaping the initial community, but also in explaining the temporal variation
311 observed in the microbial communities associated to soybean [68]and other plants [72, 73].
312 Additionally, at the maturation stage, phylogenetic null models indicated that the community was
313 neither dominated by niche-based nor by neutral processes. This shift in the community assembly
314 processes suggests changes in plant metabolic quality, i.e. decrease in metabolites supplied to
315 microbial symbiont as the plant enters senescence [74, 75]. Here, we propose that the influence of
316 niche-based processes on abundance and distribution of microbes at this stage, as shown by SDMs,

may be a relic of previous environmental selection perpetuated by microbe-microbe interaction, as previously highlighted in the rhizosphere of desert plants [76].

Our study highlighted the difficulty in getting clear data on community assembly when considering niche space to be the same in different plant compartments, suggesting that modelling community assembly across space and time is far from trivial and would require some sort of normalization for volume and population size across compartments. With that cautionary note in mind, we were still able to demonstrate that seemingly complementing approaches to quantifying assembly do reveal the dominance of niche-based processes across spatial and temporal axes. Both classes of models indicated that the plant compartment and developmental stage modulate the balance between niche-based and neutral processes. Dispersal limitations did have some influence at some specific growth stages or in defined compartments. These stages and compartments might be more readily amenable to inoculation or other microbiome manipulation approaches, as communities under stringent niche-based assembly processes are probably challenging to displace. This knowledge could orient the ongoing efforts to manipulate plant microbiomes for increased beneficial services and more sustainable agriculture.

Acknowledgements

The authors would like to thank Benjamin Mimee from Agriculture and Agri-Food Canada for providing the seeds used in the study. This work was supported by a Discovery Grant from the Natural Sciences and Engineering Research Council (NSERC) grant RGPIN 2014-05274 to EY. IM was supported by the Innovation and Scarce Skills scholarship from South African National Research Foundation (NRF), Fonds de Recherche du Québec (FRQNT), and partly by Foundation Armand-Frappier. We also wish to acknowledge Compute Canada for access to the University of Waterloo's High-Performance Computing (HPC) infrastructure (Graham system) through a resources allocation granted to EY.

Conflict of interest

The authors declare no conflict of interest.

Uncategorized References

1. Cordovez V, Dini-Andreote F, Carrion VJ, Raaijmakers JM (2019) Ecology and Evolution of Plant Microbiomes. Annu Rev Microbiol 73: 69-+. doi: 10.1146/annurev-micro-090817-062524
2. Bell TH, Hockett KL, Alcalá-Briseño RI, Barbercheck M, Beattie GA, Bruns MA, Carlson JE, Chung T, Collins A, Emmett B (2019) Manipulating wild and tamed phytobiomes: Challenges and opportunities. Phytobiomes Journal 3: 3-21.
3. Toju H, Peay KG, Yamamichi M, Narisawa K, Hiruma K, Naito K, Fukuda S, Ushio M, Nakaoka S, Onoda Y, Yoshida K, Schlaeppi K, Bai Y, Sugiura R, Ichihashi Y, Minamisawa K, Kiers ET (2018) Core microbiomes for sustainable agroecosystems. Nat Plants 4: 247-257. doi: 10.1038/s41477-018-0139-4
4. Jiao S, Yang YF, Xu YQ, Zhang J, Lu YH (2020) Balance between community assembly processes mediates species coexistence in agricultural soil microbiomes across eastern China. Isme Journal 14: 202-216. doi: 10.1038/s41396-019-0522-9
5. Vellend M (2010) Conceptual Synthesis in Community Ecology. Q Rev Biol 85: 183-206.
6. Nemergut DR, Schmidt SK, Fukami T, O'Neill SP, Bilinski TM, Stanish LF, Knelman JE, Darcy JL, Lynch RC, Wickey P, Ferrenberg S (2013) Patterns and Processes of Microbial Community Assembly. Microbiology and Molecular Biology Reviews 77: 342-356. doi: 10.1128/mmbr.00051-12
7. Wagner MR, Lundberg DS, del Rio TG, Tringe SG, Dangl JL, Mitchell-Olds T (2016) Host genotype and age shape the leaf and root microbiomes of a wild perennial plant. Nature communications 7. doi: ARTN 12151
10.1038/ncomms12151
8. Fitzpatrick CR, Copeland J, Wang PW, Guttman DS, Kotanen PM, Johnson MTJ (2018) Assembly and ecological function of the root microbiome across angiosperm plant species. P Natl Acad Sci USA 115: E1157-E1165. doi: 10.1073/pnas.1717617115
9. Dakora FD, Phillips DA (2002) Root exudates as mediators of mineral acquisition in low-nutrient environments. Plant Soil 245: 35-47. doi: Doi 10.1023/A:1020809400075
10. Hartmann A, Schmid M, Van Tuinen D, Berg G (2009) Plant-driven selection of microbes. Plant Soil 321: 235-257.
11. Perez-Jaramillo JE, Mendes R, Raaijmakers JM (2016) Impact of plant domestication on rhizosphere microbiome assembly and functions. Plant Mol Biol 90: 635-644. doi: 10.1007/s11103-015-0337-7
12. Matthews A, Pierce S, Hipperson H, Raymond B (2019) Rhizobacterial Community Assembly Patterns Vary Between Crop Species. Frontiers in Microbiology 10. doi: ARTN 581
10.3389/fmicb.2019.00581
13. Webb CO, Ackerly DD, McPeek MA, Donoghue MJ (2002) Phylogenies and community ecology. Annual Review of Ecology and Systematics 33: 475-505. doi: 10.1146/annurev.ecolysis.33.010802.150448
14. Fine PVA, Kembel SW (2011) Phylogenetic community structure and phylogenetic turnover across space and edaphic gradients in western Amazonian tree communities. Ecography 34: 552-565. doi: 10.1111/j.1600-0587.2010.06548.x

15. Stegen JC, Lin XJ, Fredrickson JK, Chen XY, Kennedy DW, Murray CJ, Rockhold ML, Konopka A (2013) Quantifying community assembly processes and identifying features that impose them. Isme Journal 7: 2069-2079. doi: 10.1038/ismej.2013.93
16. Stegen JC, Lin XJ, Konopka AE, Fredrickson JK (2012) Stochastic and deterministic assembly processes in subsurface microbial communities. Isme Journal 6: 1653-1664. doi: Doi 10.1038/Ismej.2012.22
17. Hardy OJ (2008) Testing the spatial phylogenetic structure of local communities: statistical performances of different null models and test statistics on a locally neutral community. J Ecol 96: 914-926. doi: 10.1111/j.1365-2745.2008.01421.x
18. Kembel SW (2009) Disentangling niche and neutral influences on community assembly: assessing the performance of community phylogenetic structure tests. Ecol Lett 12: 949-960. doi: 10.1111/j.1461-0248.2009.01354.x
19. Wang JJ, Shen J, Wu YC, Tu C, Soininen J, Stegen JC, He JZ, Liu XQ, Zhang L, Zhang EL (2013) Phylogenetic beta diversity in bacterial assemblages across ecosystems: deterministic versus stochastic processes. Isme Journal 7: 1310-1321. doi: 10.1038/ismej.2013.30
20. Dini-Andreote F, Stegen JC, van Elsas JD, Salles JF (2015) Disentangling mechanisms that mediate the balance between stochastic and deterministic processes in microbial succession. P Natl Acad Sci USA 112: E1326-E1332. doi: 10.1073/pnas.1414261112
21. Tripathi BM, Stegen JC, Kim M, Dong K, Adams JM, Lee YK (2018) Soil pH mediates the balance between stochastic and deterministic assembly of bacteria. Isme Journal 12: 1072-1083. doi: 10.1038/s41396-018-0082-4
22. Moroenyane I, Chimphango SBM, Wang J, Kim H-K, Adams JM (2016) Deterministic assembly processes govern bacterial community structure in the Fynbos, South Africa. Microb Ecol. doi: 10.1007/s00248-016-0761-5
23. Moroenyane I, Dong K, Singh D, Chimphango SBM, Adams JM (2016) Deterministic processes dominate nematode community structure in the Fynbos Mediterranean heathland of South Africa. Evolutionary Ecology 30: 685-701. doi: 10.1007/s10682-016-9837-4
24. Dumbrell AJ, Nelson M, Helgason T, Dytham C, Fitter AH (2010) Relative roles of niche and neutral processes in structuring a soil microbial community (vol 4, pg 337, 2010). Isme Journal 4: 1078-1078. doi: 10.1038/ismej.2010.48
25. MacArthur RH (1957) On the relative abundance of bird species. Proceedings of the National Academy of Sciences 43: 293-295.
26. Chen YH (2014) Species Abundance Distribution Pattern of Microarthropod Communities in SW Canada. Pak J Zool 46: 1023-1028.
27. Tokeshi M (1990) Niche Apportionment or Random Assortment - Species Abundance Patterns Revisited. J Anim Ecol 59: 1129-1146. doi: Doi 10.2307/5036
28. Tokeshi M (1993) Species Abundance Patterns and Community Structure. Adv Ecol Res 24: 111-186. doi: Doi 10.1016/S0065-2504(08)60042-2
29. Sugihara G (1980) Minimal Community Structure - an Explanation of Species Abundance Patterns. Am Nat 116: 770-787. doi: Doi 10.1086/283669
30. Etienne RS, Olff H (2005) Confronting different models of community structure to species-abundance data: a Bayesian model comparison. Ecol Lett 8: 493-504. doi: 10.1111/j.1461-0248.2005.00745.x

31. Hubbell SP (2001) The unified neutral theory of biodiversity and biogeography. Princeton University Press, Princeton
32. McGill BJ (2003) A test of the unified neutral theory of biodiversity. Nature 422: 881-885. doi: 10.1038/nature01583
33. Moroenyane I, Chimphango S, Dong K, Tripathi B, Singh D, Adams J (2019) Neutral models predict biogeographical patterns of soil microbes at a local scale in Mediterranean heathlands, South Africa. Transactions of the Royal Society of South Africa 1-12. doi: doi.org/10.1080/0035919X.2019.1603126
34. Goss-Souza D, Mendes LW, Rodrigues JLM, Tsai SM (2019) Ecological Processes Shaping Bulk Soil and Rhizosphere Microbiome Assembly in a Long-Term Amazon Forest-to-Agriculture Conversion. Microb Ecol. doi: 10.1007/s00248-019-01401-y
35. Mendes LW, Kuramae EE, Navarrete AA, van Veen JA, Tsai SM (2014) Taxonomical and functional microbial community selection in soybean rhizosphere. Isme Journal 8: 1577-1587. doi: 10.1038/ismej.2014.17
36. Feinstein LM, Blackwood CB (2012) Taxa-area relationship and neutral dynamics influence the diversity of fungal communities on senesced tree leaves. Environ Microbiol 14: 1488-1499. doi: 10.1111/j.1462-2920.2012.02737.x
37. Moscatiello R, Baldan B, Navazio L (2013) Plant cell suspension cultures. Methods Mol Biol 953: 77-93. doi: 10.1007/978-1-62703-152-3_5
38. Qvit-Raz N, Jurkevitch E, Belkin S (2008) Drop-size soda lakes: Transient microbial habitats on a salt-secreting desert tree. Genetics 178: 1615-1622. doi: 10.1534/genetics.107.082164
39. Edwards JE, Kingston-Smith AH, Jimenez HR, Huws SA, Skot KP, Griffith GW, McEwan NR, Theodorou MK (2008) Dynamics of initial colonization of nonconserved perennial ryegrass by anaerobic fungi in the bovine rumen. Fems Microbiol Ecol 66: 537-545. doi: 10.1111/j.1574-6941.2008.00563.x
40. Tremblay J, Singh K, Fern A, Kirton ES, He S, Woyke T, Lee J, Chen F, Dangl JL, Tringe SG (2015) Primer and platform effects on 16S rRNA tag sequencing. Front Microbiol 6: 771. doi: 10.3389/fmicb.2015.00771
41. Tremblay J, Yergeau E (2019) Systematic processing of ribosomal RNA gene amplicon sequencing data. GigaScience 8. doi: 10.1093/gigascience/giz146
42. Magoc T, Salzberg SL (2011) FLASH: fast length adjustment of short reads to improve genome assemblies. Bioinformatics 27: 2957-2963. doi: 10.1093/bioinformatics/btr507
43. Ghodsi M, Liu B, Pop M (2011) DNACLUST: accurate and efficient clustering of phylogenetic marker genes. Bmc Bioinformatics 12: 271. doi: 10.1186/1471-2105-12-271
44. Rognes T, Flouri T, Nichols B, Quince C, Mahe F (2016) VSEARCH: a versatile open source tool for metagenomics. Peerj 4: e2584. doi: 10.7717/peerj.2584
45. Edgar RC, Haas BJ, Clemente JC, Quince C, Knight R (2011) UCHIME improves sensitivity and speed of chimera detection. Bioinformatics 27: 2194-2200. doi: 10.1093/bioinformatics/btr381
46. Wang Q, Garrity GM, Tiedje JM, Cole JR (2007) Naive Bayesian classifier for rapid assignment of rRNA sequences into the new bacterial taxonomy. Appl Environ Microbiol 73: 5261-5267.
47. Tremblay J (2019) AmpliconTagger pipeline databases (Version 1).

48. Quast C, Pruesse E, Yilmaz P, Gerken J, Schweer T, Yarza P, Peplies J, Glockner FO (2013) The SILVA ribosomal RNA gene database project: improved data processing and web-based tools. Nucleic Acids Res 41: D590-D596. doi: 10.1093/nar/gks1219
49. Caporaso JG, Kuczynski J, Stombaugh J, Bittinger K, Bushman FD, Costello EK, Fierer N, Pena AG, Goodrich JK, Gordon JI, Huttley GA, Kelley ST, Knights D, Koenig JE, Ley RE, Lozupone CA, McDonald D, Muegge BD, Pirrung M, Reeder J, Sevinsky JR, Turnbaugh PJ, Walters WA, Widmann J, Yatsunenko T, Zaneveld J, Knight R (2010) QIIME allows analysis of high-throughput community sequencing data. Nat Methods 7: 335-336. doi: 10.1038/nmeth.f.303
50. Kuczynski J, Stombaugh J, Walters WA, González A, Caporaso JG, Knight R (2011) Using QIIME to analyze 16S rRNA gene sequences from microbial communities. Current protocols in bioinformatics 36: 10.17. 11-10.17. 20.
51. Caporaso JG, Kuczynski J, Stombaugh J, Bittinger K, Bushman FD, Costello EK, Fierer N, Pena AG, Goodrich JK, Gordon JI, Huttley GA, Kelley ST, Knights D, Koenig JE, Ley RE, Lozupone CA, McDonald D, Muegge BD, Pirrung M, Reeder J, Sevinsky JR, Tumbaugh PJ, Walters WA, Widmann J, Yatsunenko T, Zaneveld J, Knight R (2010) QIIME allows analysis of high-throughput community sequencing data. Nat Methods 7: 335-336. doi: 10.1038/nmeth.f.303
52. Oksanen J, Blanchet FG, Kindt R, Legendre P, Minchin PR, O'Hara R, Simpson GL, Solymos P, Stevens MHH, Wagner H (2013) Package 'vegan'. Community ecology package, version 2.
53. Jabot F, Etienne RS, Chave J (2008) Reconciling neutral community models and environmental filtering: theory and an empirical test. Oikos 117: 1308-1320. doi: 10.1111/j.2008.0030-1299.16724.x
54. Dumbrell AJ, Nelson M, Helgason T, Dytham C, Fitter AH (2010) Relative roles of niche and neutral processes in structuring a soil microbial community. Isme Journal 4: 337-345. doi: 10.1038/ismej.2009.122
55. Burnham KP, Anderson DR (2003) Model selection and multimodel inference: a practical information-theoretic approach. Springer Science & Business Media
56. Price MN, Dehal PS, Arkin AP (2010) FastTree 2-Approximately Maximum-Likelihood Trees for Large Alignments. Plos One 5. doi: ARTN e9490
10.1371/journal.pone.0009490
57. Kembel SW, Cowan PD, Helmus MR, Cornwell WK, Morlon H, Ackerly DD, Blomberg SP, Webb CO (2010) Picante: R tools for integrating phylogenies and ecology. Bioinformatics 26: 1463-1464. doi: 10.1093/bioinformatics/btq166
58. Stegen JC, Lin X, Fredrickson JK, Konopka AE (2015) Estimating and mapping ecological processes influencing microbial community assembly. Front Microbiol 6: 370. doi: 10.3389/fmicb.2015.00370
59. Moroenyane I, Tremblay J, Yergeau É (2020) Temporal and spatial interactions modulate the soybean microbiome. Fems Microbiol Ecol.
60. Miller ET, Farine DR, Trisos CH (2017) Phylogenetic community structure metrics and null models: a review with new methods and software. Ecography 40: 461-477. doi: 10.1111/ecog.02070
61. Rengel Z, Marschner P (2005) Nutrient availability and management in the rhizosphere: exploiting genotypic differences. New Phytol 168: 305-312. doi: 10.1111/j.1469-8137.2005.01558.x

62. Chase JM (2010) Stochastic Community Assembly Causes Higher Biodiversity in More Productive Environments. Science 328: 1388-1391. doi: 10.1126/science.1187820
63. Smalla K, Wieland G, Buchner A, Zock A, Parzy J, Kaiser S, Roskot N, Heuer H, Berg G (2001) Bulk and rhizosphere soil bacterial communities studied by denaturing gradient gel electrophoresis: plant-dependent enrichment and seasonal shifts revealed. Appl Environ Microbiol 67: 4742-4751.
64. Langenheder S, Szekely AJ (2011) Species sorting and neutral processes are both important during the initial assembly of bacterial communities. Isme Journal 5: 1086-1094. doi: 10.1038/ismej.2010.207
65. Maignien L, DeForce EA, Chafee ME, Eren AM, Simmons SL (2014) Ecological succession and stochastic variation in the assembly of Arabidopsis thaliana phyllosphere communities. mBio 5: e00682-00613. doi: 10.1128/mBio.00682-13
66. Subramanian S, Cho UH, Keyes C, Yu O (2009) Distinct changes in soybean xylem sap proteome in response to pathogenic and symbiotic microbe interactions. BMC plant biology 9: 119. doi: 10.1186/1471-2229-9-119
67. Ikeda S, Okubo T, Kaneko T, Inaba S, Maekawa T, Eda S, Sato S, Tabata S, Mitsui H, Minamisawa K (2010) Community shifts of soybean stem-associated bacteria responding to different nodulation phenotypes and N levels. The ISME journal 4: 315-326.
68. Hara S, Matsuda M, Minamisawa K (2019) Growth Stage-dependent Bacterial Communities in Soybean Plant Tissues: Methylorubrum Transiently Dominated in the Flowering Stage of the Soybean Shoot. Microbes and environments 34: 446-450. doi: 10.1264/jsme2.ME19067
69. Copeland JK, Yuan LJ, Layeghifard M, Wang PW, Guttman DS (2015) Seasonal Community Succession of the Phyllosphere Microbiome. Mol Plant Microbe In 28: 274-285. doi: 10.1094/Mpmi-10-14-0331-Fi
70. Zhang BG, Zhang J, Liu Y, Shi P, Wei GH (2018) Co-occurrence patterns of soybean rhizosphere microbiome at a continental scale. Soil Biol Biochem 118: 178-186. doi: 10.1016/j.soilbio.2017.12.011
71. Liu F, Hewezi T, Lebeis SL, Pantalone V, Grewal PS, Staton ME (2019) Soil indigenous microbiome and plant genotypes cooperatively modify soybean rhizosphere microbiome assembly. Bmc Microbiol 19: 201. doi: 10.1186/s12866-019-1572-x
72. Chaparro JM, Badri DV, Vivanco JM (2014) Rhizosphere microbiome assemblage is affected by plant development. Isme Journal 8: 790-803. doi: 10.1038/ismej.2013.196
73. Amend AS, Cobian GM, Laruson AJ, Remple K, Tucker SJ, Poff KE, Antaky C, Boraks A, Jones CA, Kuehu D, Lensing BR, Pejhanmehr M, Richardson DT, Riley PP (2019) Phytobiomes are compositionally nested from the ground up. Peerj 7. doi: ARTN e6609 10.7717/peerj.6609
74. Zhalnina K, Louie KB, Hao Z, Mansoori N, da Rocha UN, Shi SJ, Cho HJ, Karaoz U, Loque D, Bowen BP, Firestone MK, Northen TR, Brodie EL (2018) Dynamic root exudate chemistry and microbial substrate preferences drive patterns in rhizosphere microbial community assembly. Nature Microbiology 3: 470-480. doi: 10.1038/s41564-018-0129-3
75. Bell CW, Asao S, Calderon F, Wolk B, Wallenstein MD (2015) Plant nitrogen uptake drives rhizosphere bacterial community assembly during plant growth. Soil Biol Biochem 85: 170-182. doi: 10.1016/j.soilbio.2015.03.006

76. Marasco R, Mosqueira MJ, Fusi M, Ramond JB, Merlino G, Booth JM, Maggs-Kolling G, Cowan DA, Daffonchio D (2018) Rhizosheath microbial community assembly of sympatric desert speargrasses is independent of the plant host. Microbiome 6. doi: ARTN 215
10.1186/s40168-018-0597-y

Table and Figures

Fig.1 Boxplot of βNTI observations across plant compartments, where each observation is the number of null model standard deviations the observed value is from the mean of null distribution. The dashed blue lines indicate the significant upper and lower limits thresholds of βNTI at +2 and -2. A t-test was performed on the mean value of the βNTI to test if it significantly deviated from zero which is expected under neutral assembly: Leaf (Endophyte μ = -0.52*; Epiphyte μ = -0.21***), Stem (Endophyte μ = -0.64***; Epiphyte μ = -1.01***), Root (Endophyte μ = -0.82***; Epiphyte μ = -0.76***), and Rhizosphere (μ = -0.14*;)Where * indicates significance level (*<0.05; **<0.001, ***<0.0001)**

Fig.2 Bacterial community assembly processes (across plant organs) of fitted rank abundance models; models with lowest Akaike Information Criterion (AIC) values were best fit. AIC values were calculated from the equation: $AIC = -2loglikelihood + 2 * npar$

Fig.3 The percentage of dispersal in community assembly and dispersal rates were calculated using TeTame software with Etienne's formula, where *m* values are between 0 and 1. When *m*=1 indicates increased tendency to migrate and *m*=0 indicates no tendency to migrate across plant compartment.

Fig.4 Boxplot of βNTI observations across developmental stages, where each observation is the number of null model standard deviations the observed value is from the mean of null

distribution. The dashed blue lines indicate significant upper and lower limits thresholds of βNTI at +2 and -2. A t-test was performed on the mean value of the βNTI to test if it significantly deviated from zero which is expected under neutral assembly: Emerging (μ = -0.21*), Growth (μ = -0.19***), Flowering (μ = -0.23***), Maturation (μ = -0.07***), and Overall (μ = -0.70). Where * indicates significance level (*<0.05; **<0.001, ***<0.0001)**

Fig. 5 The percentage of turnover in community assembly modulated by various niche-based (homogenous and heterogeneous selection), neutral processes (dispersal limitation and homogenising dispersal), and a fraction that was not dominated by any process across developmental stages.

Fig.6 Bacterial community assembly processes (across developmental stages) of fitted rank abundance models; models with lowest Akaike Information Criterion (AIC) values were best fit. AIC values were calculated from the equation: $AIC = -2loglikelihood + 2 * npar$

Figure 1

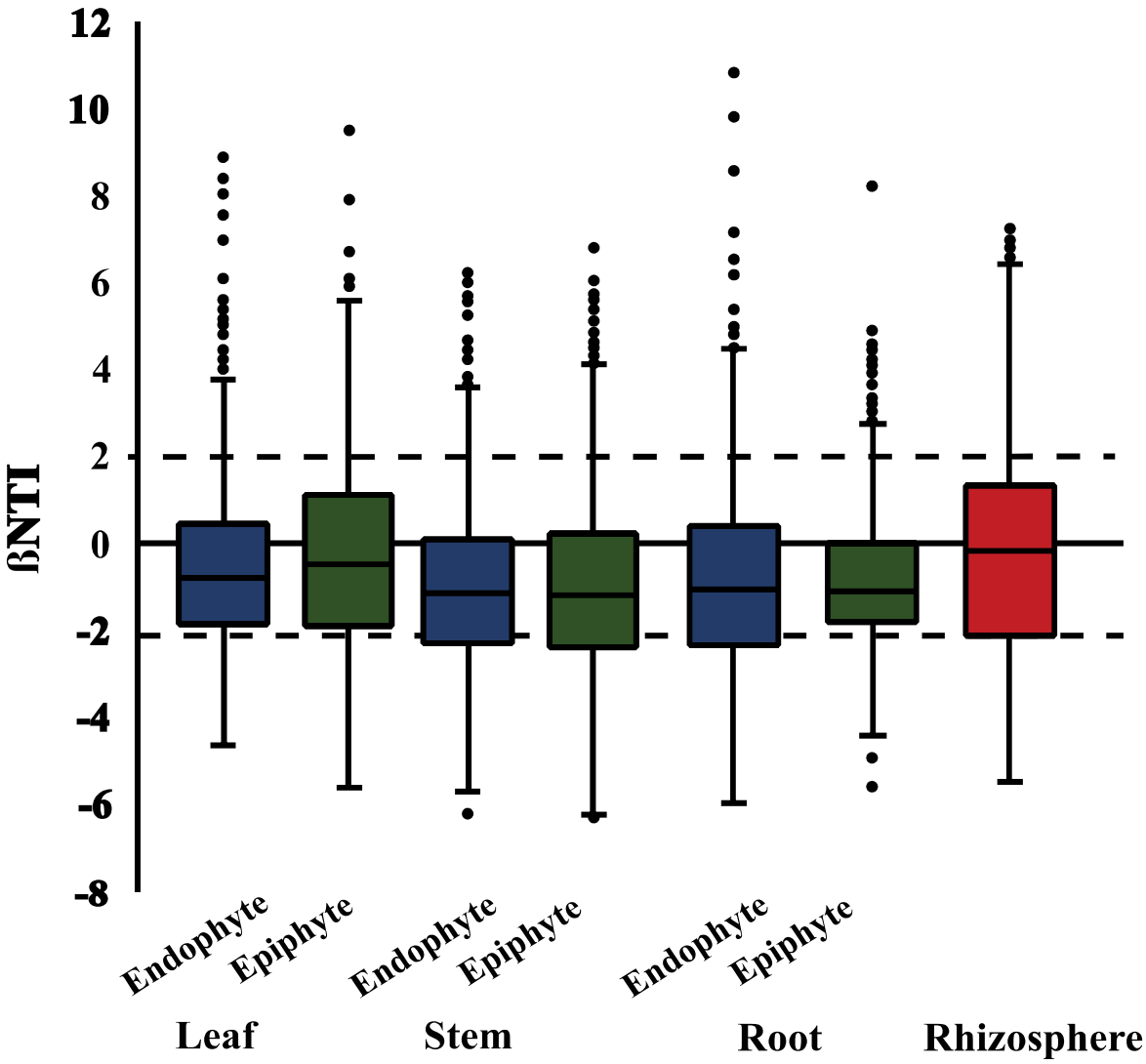

Fig.1 Boxplot of βNTI observations across plant compartments, where each observation is the number of null model standard deviations the observed value is from the mean of null distribution. The dashed blue lines indicate the significant upper and lower limits thresholds of βNTI at +2 and -2. A t-test was performed on the mean value of the βNTI to test if it significantly deviated from zero which is expected under neutral assembly: Leaf (Endophyte μ = -0.52*; Epiphyte μ = -0.21***), Stem (Endophyte μ = -0.64***; Epiphyte μ = -1.01***), Root (Endophyte μ = -0.82***; Epiphyte μ = -0.76***), and Rhizosphere (μ = -0.14*;)Where * indicates significance level (*<0.05; **<0.001, ***<0.0001)**

Figure 2

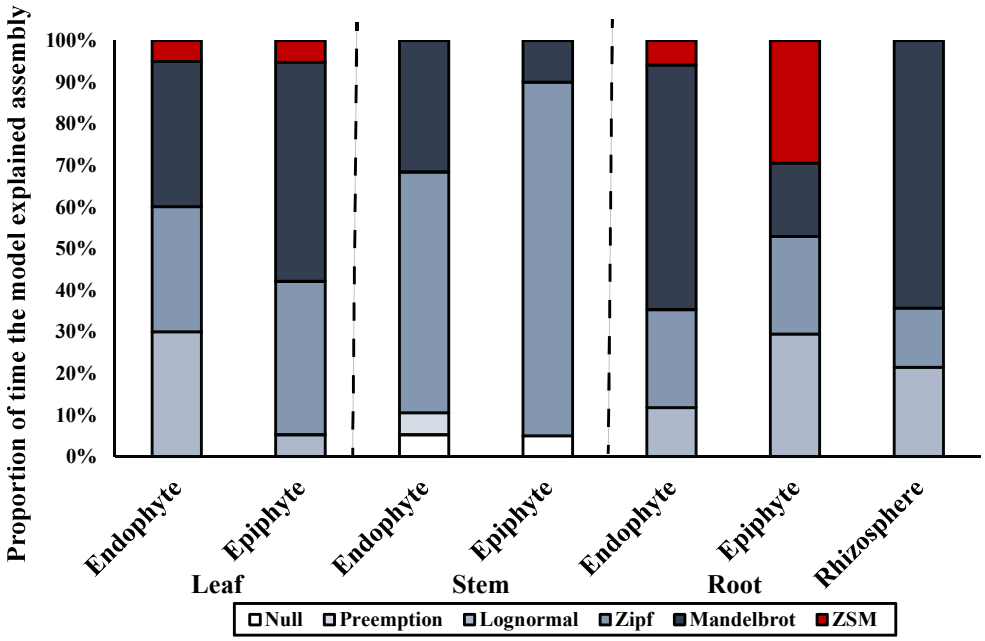

Fig.2 Bacterial community assembly processes (across plant organs) of fitted rank abundance models; models with lowest Akaike Information Criterion (AIC) values were best fit. AIC values were calculated from the equation: $AIC = -2loglikelihood + 2 * npar$

Figure 3

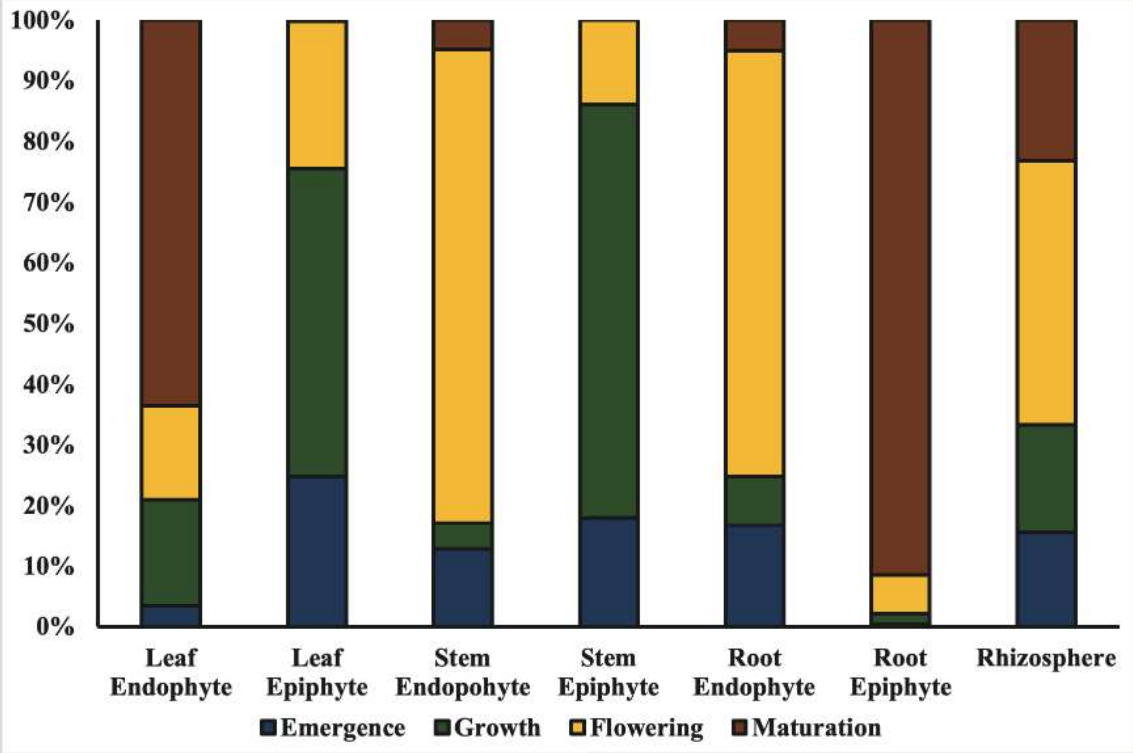

Fig.3 The percentage of dispersal in community assembly and dispersal rates were calculated using TeTame software with Etienne's formula, where *m* values are between 0 and 1. When *m*=1 indicates increased tendency to migrate and *m*=0 indicates no tendency to migrate across plant compartment.

Figure 4

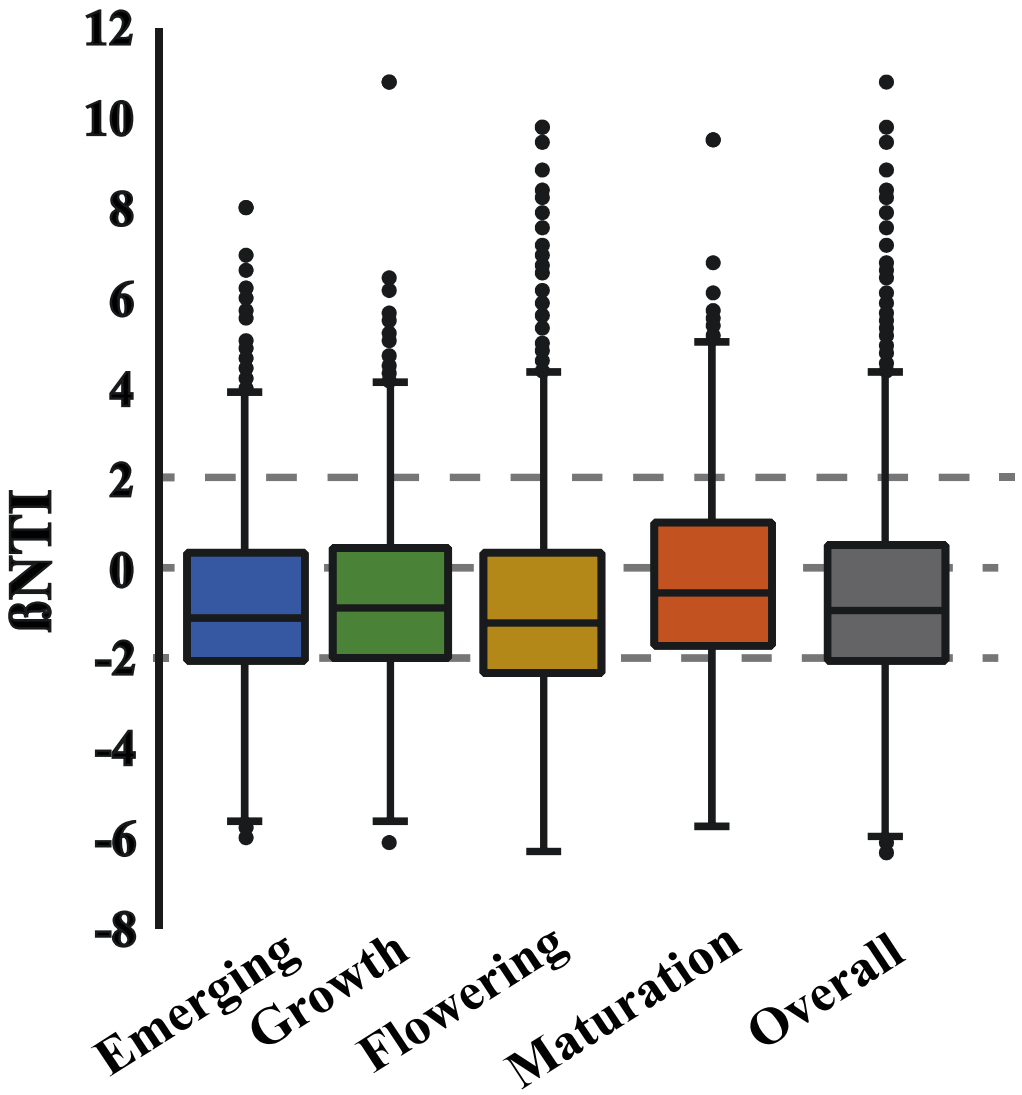

Fig.4 Boxplot of βNTI observations across developmental stages, where each observation is the number of null model standard deviations the observed value is from the mean of null distribution. The dashed blue lines indicate significant upper and lower limits thresholds of βNTI at +2 and -2. A t-test was performed on the mean value of the βNTI to test if it significantly deviated from zero which is expected under neutral assembly: Emerging (μ = -0.21*), Growth (μ = -0.19***), Flowering (μ = -0.23***), Maturation (μ = -0.07***), and Overall (μ = -0.70). Where * indicates significance level (*<0.05; **<0.001, ***<0.0001)**

Figure 5

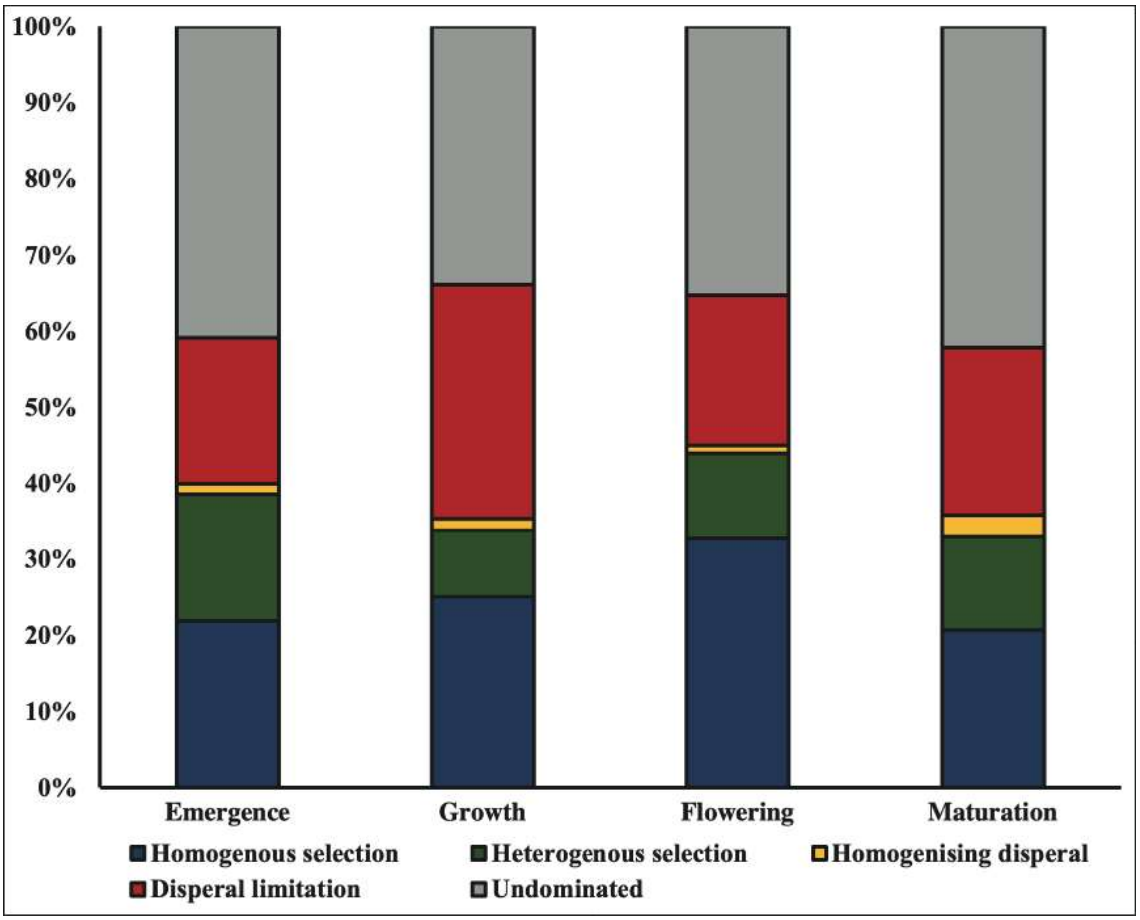

Fig. 5 The percentage of turnover in community assembly modulated by various niche-based (homogenous and heterogeneous selection), neutral processes (dispersal limitation and homogenising dispersal), and a fraction that was not dominated by any process across developmental stages.

Figure 6

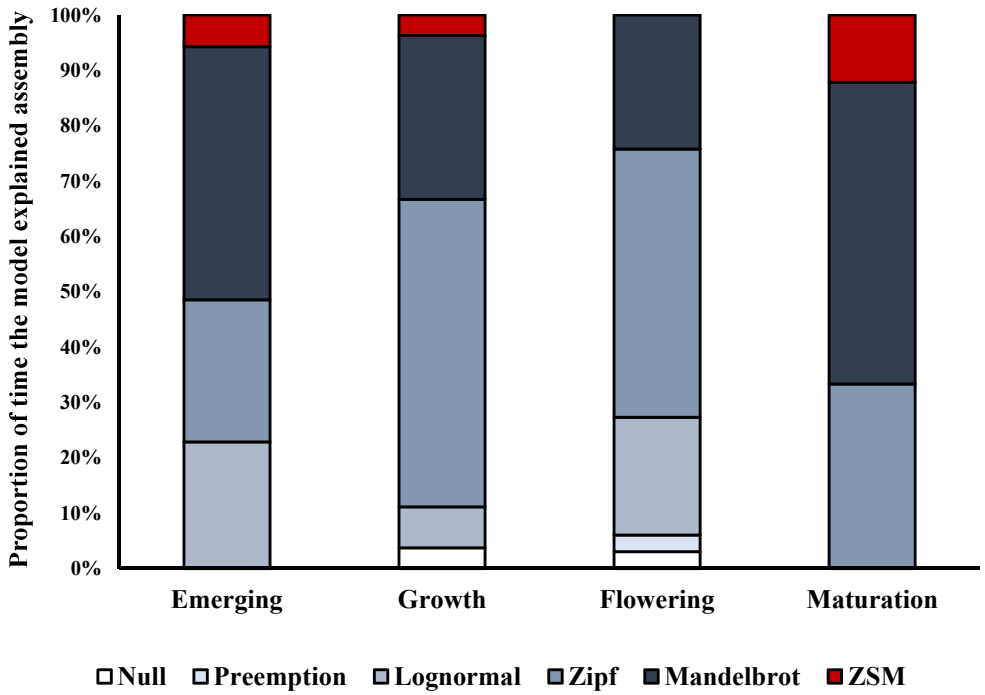

Fig.6 Bacterial community assembly processes (across developmental stages) of fitted rank abundance models; models with lowest Akaike Information Criterion (AIC) values were best fit. AIC values were calculated from the equation: $AIC = -2loglikelihood + 2 * npar$

Table 1

Table 1. Bacterial Akaike Information Criterion (AIC) values of fitted rank abundance models. models with lowest Akaike Information Criterion (AIC) values were best fit. AIC values were calculated from the equation: $AIC = -2loglikelihood + 2 * npar$

			Akaike Information criterion (AIC)					
			Niche-based					Neutral
Organ	**Developmental stage**	**ID**	**Null**	**Preemption**	**Lognormal**	**Zipf**	**Mandelbrot**	**ZSM**
Leaf Endophyte	Emerging	**LE1-1**	1731.30	1636.61	**1063.21**	2057.79	1611.09	2151.64
		LE1-2	1259.84	1504.27	**1032.45**	1841.66	1453.29	2727.94
		LE1-3	4927.37	4868.88	**1573.91**	2518.82	2106.26	3785.24
		LE1-4	1675.18	1973.17	**1026.15**	1696.63	1544.46	2167.11
		LE1-5	6728.90	6915.60	**2123.10**	2694.90	2696.90	4424.70
	Growth	**LE2-1**	87015.80	39446.40	5198.60	2924.10	2926.10	**2257.24**
		LE2-2	7966.14	6809.24	2061.90	**1420.73**	1422.73	1964.87
		LE2-3	4508.65	4155.71	1519.77	**1049.60**	1051.60	1917.98
		LE2-4	6382.61	5047.45	1635.65	**1176.68**	1178.68	1559.45
		LE2-5	8214.80	7027.90	2245.40	**1572.40**	1574.40	2018.11
	Flowering	**LE3-1**	7277.60	3059.96	1126.86	1301.90	**767.68**	2633.86
		LE3-2	1671.15	1182.84	696.00	767.64	**550.13**	2261.44
		LE3-3	5405.77	4206.96	1192.67	**824.27**	826.27	1952.84
		LE3-4	537.73	597.40	466.02	**457.51**	459.18	1931.33
		LE3-5	673.46	719.96	**504.30**	608.39	542.89	2033.88
	Maturation	**LE4-1**	159.64	147.87	143.62	147.56	**132.80**	587.88
		LE4-2	280.67	290.54	252.62	243.32	**242.59**	1238.01
		LE4-3	445.21	474.87	385.28	370.36	**370.15**	1776.41
		LE4-4	515.30	535.25	382.43	347.64	**344.61**	1611.13

		LE4-5	239.03	235.14	222.83	221.16	**211.52**	1034.02
Leaf Epiphyte	Emerging	**LP1-1**	3453.59	3079.55	**1034.68**	1308.73	1310.73	3701.28
		LP1-2	169466.70	103572.90	15741.00	22986.80	NA	30959.80
		LP1-3	2468.73	2655.96	1352.99	**980.06**	982.06	3715.44
		LP1-4	501.13	512.65	381.30	338.84	**333.81**	1131.84
		LP1-5	51.54	47.80	44.24	**40.23**	42.23	186.31
	Growth	**LP2-1**	268.90	273.13	241.04	**222.59**	224.59	934.96
		LP2-2	23329.42	15662.00	3742.96	4127.47	**3187.77**	11376.68
		LP2-3	72.63	65.04	64.64	**62.46**	64.46	264.43
		LP2-4	132.36	120.38	111.37	116.40	**105.40**	419.49
		LP2-5	5917.21	4898.46	1668.12	1477.03	**1431.80**	5399.24
	Flowering	**LP3-1**	354.22	375.78	283.29	**237.85**	239.85	1086.25
		LP3-2	5337.65	3311.12	1059.60	**810.88**	812.88	1669.41
		LP3-3	224851.50	135978.60	10801.70	**5252.60**	5254.60	14874.92
		LP3-4	1739.63	1713.25	1129.09	1053.90	**949.51**	3577.40
		LP3-5	1973.75	1313.77	506.37	448.44	**412.82**	1666.46
	Maturation	**LP4-1**	116559.34	39012.06	3792.50	2946.54	**1960.75**	4721.30
		LP4-2	119928.30	36207.90	4763.70	3943.40	**3103.20**	4516.82
		LP4-3	49065.20	15185.40	3559.40	2884.50	**2191.40**	4789.04
		LP4-4	98097.00	23961.70	5364.30	5035.00	**2297.60**	6583.98
		LP4-5	45729.30	6258.10	5801.50	5962.80	3433.80	**2603.98**
Rhizosphere	Emerging	**R1-1**	20321.87	14809.94	7647.61	11695.92	**6704.83**	26104.20
		R1-2	9511.84	8118.59	4655.16	5932.30	**4314.59**	16121.94
		R1-3	47410.60	30584.00	10043.00	17440.50	NA	33673.20
		R1-4	46179.30	26828.40	10376.60	19500.10	NA	30958.80
		R1-5	16426.03	12405.64	6058.69	8738.74	**5853.93**	20814.50
	Growth	**R2-1**	41114.00	26828.60	8669.80	13987.40	NA	26697.80

		R2-2	56672.70	35468.50	11192.80	19230.20	NA	33378.60
		R2-3	12999.95	10448.33	5218.17	6893.44	**4773.15**	17314.98
		R2-4	4433.89	4253.87	2869.86	3178.24	**2653.35**	10115.56
		R2-5	49580.70	32668.20	9212.10	14600.40	NA	29040.20
	Flowering	**R3-1**	3160622.00	1724628.00	**67308.00**	92921.00	71980.00	73263.80
		R3-2	49.59	46.14	46.42	**44.67**	46.67	189.52
		R3-3	53947.70	30172.70	**12119.60**	23416.30	NA	33513.40
		R3-4	36796.10	31072.40	6960.60	**5443.90**	5445.90	13551.96
		R3-5	71502.90	45460.90	**8790.30**	13409.60	9315.70	23072.62
	Maturation	**R4-1**	87471.70	43841.50	17177.80	35477.10	NA	40397.20
		R4-2	3965.95	3930.50	2742.17	2951.24	**2547.70**	10118.84
		R4-3	13248.83	10139.84	5476.08	7514.48	**4981.22**	18473.70
		R4-4	17526.94	12942.67	6501.00	9229.46	**5658.92**	21676.72
		R4-5	23039.70	16685.50	5006.00	6359.60	**4743.60**	14187.52
Root Endophyte	Emerging	**RE1-1**	146354.40	76607.80	**7897.20**	11146.90	7947.10	19471.42
		RE1-2	1370.25	1340.06	758.77	**674.32**	675.92	2911.30
		RE1-3	20902.04	15263.92	3208.38	2501.23	**2343.76**	8547.12
		RE1-4	21411.70	13445.55	2967.40	3375.03	**2455.53**	9737.94
		RE1-5	13658.32	7898.62	3173.42	4789.58	**2403.20**	10172.64
	Growth	**RE2-1**	13370.81	7468.01	2613.56	3820.23	**2093.86**	8398.82
		RE2-2	22746.25	12710.13	3523.70	5213.65	**2688.32**	11384.34
		RE2-3	77678.60	31970.60	8343.10	15038.30	NA	15894.94
		RE2-4	37042.26	20805.52	3820.10	4827.30	**2869.46**	11608.16
		RE2-5	60672.40	28841.80	8044.70	13572.50	NA	17154.74
	Flowering	**RE3-1**	39375.78	25257.11	3278.44	**2444.07**	2446.07	8513.28
		RE3-2	73251.70	37916.20	**4272.60**	6508.50	5037.10	15300.64
		RE3-3	29.66	**27.86**	28.99	28.56	30.56	144.54

		RE3-4	35973.80	23017.40	3751.90	4135.70	**3675.20**	13186.74
		RE3-5	8248.63	5632.40	1801.59	1868.45	**1440.65**	6611.90
	Maturation	**RE4-1**	4195.19	3220.01	897.99	**593.40**	595.40	2861.04
		RE4-2	16427.30	4088.10	3376.10	5436.10	2255.20	**1876.60**
		RE4-3	147576.20	87397.90	14241.20	**9752.80**	9754.80	10994.52
		RE4-4	34640.62	22271.40	3890.23	2992.94	**2500.59**	9438.72
		RE4-5	17734.20	9474.50	2319.90	2203.70	**1829.90**	3447.56
Root Epiphyte	Emerging	**RP1-1**	104897.90	31644.80	3469.70	**1916.80**	1918.80	2225.02
		RP1-2	34518.20	10558.80	3661.40	6927.30	5677.50	**1710.09**
		RP1-3	121813.80	69599.20	8014.60	5366.00	**4859.80**	11663.26
		RP1-4	7467.70	6849.90	**3206.40**	5162.90	5164.90	4987.42
		RP1-5	75864.00	11715.40	7266.90	9161.00	6277.50	**1101.10**
	Growth	**RP2-1**	284881.00	138584.00	19381.00	30372.00	30374.00	**14825.64**
		RP2-2	105838.20	46109.50	**6829.80**	17734.50	15566.80	9980.66
		RP2-5	36322.40	17367.30	**5529.00**	15199.70	NA	16390.80
	Flowering	**RP3-1**	65812.60	31443.50	**3151.40**	4578.60	4169.20	5950.90
		RP3-2	20789.44	17338.29	4532.77	3505.16	**3207.61**	14351.18
		RP3-3	27353.80	25041.00	5857.20	**3600.90**	3602.90	7225.66
		RP3-4	5652.54	850.89	457.95	594.58	**366.96**	438.74
		RP3-5	11903.11	11242.08	**2901.61**	3080.43	3082.43	7934.16
	Maturation	**RP4-1**	39778.65	NA	578.41	**384.71**	386.71	862.00
		RP4-2	160817.00	26075.00	16549.00	14300.00	NA	**4041.64**
		RP4-3	**19.82**	21.42	22.72	21.39	23.39	85.16
		RP4-4	36.18	33.35	33.76	**32.92**	34.92	162.40
		RP4-5	53243.40	3953.90	6065.40	8679.20	NA	**3437.38**
Stem Endophyte	Emerging	**SE1-1**	22874.36	2627.93	2600.39	2920.11	**1123.27**	1695.79
		SE1-2	643.24	657.30	416.19	370.69	**365.87**	1499.59

		SE1-3	1742.77	1819.81	995.72	953.16	**884.26**	3527.46
		SE1-4	558.76	596.29	440.34	439.01	**421.40**	1612.81
		SE1-5	277.28	267.65	228.54	224.84	**209.64**	905.48
	Growth	**SE2-1**	68720.00	44720.40	5578.10	**4258.40**	4260.40	6061.14
		SE2-2	59392.30	32766.20	5150.70	**3839.90**	3841.90	6264.10
		SE2-3	49.68	47.12	42.08	**34.75**	36.75	146.82
		SE2-4	146357.20	123413.80	10741.40	**8709.60**	8711.60	8870.48
		SE2-5	14561.08	8078.75	1329.11	**773.92**	775.92	2801.10
	Flowering	**SE3-1**	13.15	**13.12**	14.00	14.00	16.00	72.16
		SE3-2	9750.87	8076.91	2265.21	**1569.14**	1571.14	4057.02
		SE3-3	8912.80	7555.40	2230.20	**1510.90**	1512.90	3947.50
		SE3-5	**10.22**	10.89	12.00	12.00	14.00	43.30
	Maturation	**SE4-1**	9931.74	7793.14	1872.30	**1196.93**	1198.93	3546.76
		SE4-2	24322.62	11803.20	1896.04	1893.60	**1133.83**	4774.00
		SE4-3	30694.20	22336.20	4075.80	**2807.70**	2809.70	6324.76
		SE4-4	19104.01	14162.74	3003.55	**2160.33**	2162.33	5867.80
		SE4-5	28519.10	23974.10	5248.40	**2944.50**	2946.50	8316.84
Stem Epiphyte	Emerging	**SP1-1**	9966.74	8050.04	2230.10	**1495.05**	1497.05	4244.22
		SP1-2	6853.10	5293.75	1514.06	**1053.47**	1055.47	3059.54
		SP1-3	11398.59	8603.62	1979.93	**1236.89**	1238.89	3814.10
		SP1-4	15320.50	12060.10	2788.30	**1780.60**	1782.60	4837.06
		SP1-5	11814.34	8919.97	2112.46	**1398.06**	1400.06	3938.26
	Growth	**SP2-1**	15898.19	12266.16	2765.02	**1712.02**	1714.02	4692.86
		SP2-2	21181.87	15766.97	3218.75	**2025.06**	2027.06	5385.90
		SP2-3	**12.70**	13.40	14.84	14.75	16.75	67.47
		SP2-4	29305.35	26887.04	6455.59	**3896.90**	3898.90	12699.78
		SP2-5	55594.30	41112.20	6428.70	**3804.00**	3806.00	8841.26

	Flowering	**SP3-1**	19746.85	15337.61	3314.05	**2022.32**	2024.32	5023.20
		SP3-2	12365.27	9677.30	2283.03	**1439.61**	1441.61	4442.32
		SP3-3	24216.64	17545.33	3432.94	**2177.00**	2179.00	5661.16
		SP3-4	17151.53	13248.13	3045.70	**1905.20**	1907.20	5151.12
		SP3-5	9455.30	7505.32	1863.38	**1160.44**	1162.44	3940.64
	Maturation	**SP4-1**	76934.07	11393.37	2497.32	2510.86	**901.79**	3230.02
		SP4-2	123765.90	12891.60	6943.20	6098.80	**2775.70**	2967.54
		SP4-3	34643.30	7384.83	1018.76	**611.51**	613.51	1965.01
		SP4-4	44753.33	8032.92	988.98	**592.04**	594.04	1952.83
		SP4-5	65893.30	18230.60	2018.50	**1646.60**	1648.60	2850.32

Table 2

Table 2. Dispersal rates across developmental stages and plant compartments of soybean-associated bacterial communities.

Organ	Developmental stage	Dispersal rate (*m*)
Leaf endophyte	Emerging	0.008
	Growth	0.041
	Flowering	0.036
	Maturation	**0.148**
Leaf epiphyte	Emerging	0.142
	Growth	**0.290**
	Flowering	0.139
	Maturation	0.001
Rhizosphere	Emerging	0.073
	Growth	0.084
	Flowering	**0.205**
	Maturation	0.109
Root endophyte	Emerging	0.033
	Growth	0.016
	Flowering	**0.139**
	Maturation	0.010
Root epiphyte	Emerging	0.001
	Growth	0.004
	Flowering	0.015
	Maturation	**0.215**
Stem endophyte	Emerging	0.087
	Growth	0.030
	Flowering	**0.531**
	Maturation	0.033
Stem epiphyte	Emerging	0.044
	Growth	**0.166**
	Flowering	0.034
	Maturation	6.17604E-07

Dispersal rates were calculated using TeTame software with Etienne's formula, where *m* values are between 0 and 1. When *m*=1 indicates increased tendency to migrate and *m*=0 indicates no tendency to migrate